

## ***In-situ* quantification of micro-segregation that occurs during the solidification of steel**

Stefan Griesser<sup>1\*</sup>, Mark Reid<sup>1</sup>, Robert Pierer<sup>2</sup>, Christian Bernhard<sup>2</sup> and Rian Dippenaar<sup>1</sup>

<sup>1</sup>*University of Wollongong, Faculty of Engineering, Wollongong, Australia*

<sup>2</sup>*University of Leoben, Chair of Metallurgy, Leoben, Austria*

*Corresponding author: e-mail sg045@uowmail.edu.au*

We present a method for the *in-situ* quantification of micro-segregation during the solidification of steel by using high-temperature laser-scanning confocal microscopy (HTLSCM). A newly developed experimental technique that has been developed for the HTLSCM has been utilized to investigate the effect of different alloying elements and cooling rates on the solidification behaviour of steel. An automated quantitative measurement of the fractions of solid and liquid during solidification is used to calculate the average phase concentrations by applying a simple mass balance. The results of these analyses are in very good agreement with simulations carried out by using the commercial software package DICTRA.

Key words: Solidification, segregation, partitioning, HTLSCM, steel.

### **Introduction**

The understanding and modelling of micro-segregation that occurs during solidification of alloys is of essential importance for the improvement and development of commercial casting processes. Within the past decades a wide range of more and less complex mathematical models has been developed as a tool to quantify the extent of microsegregation during solidification. A common limitation in all of these models is the accuracy and availability of kinetic and/or thermodynamic data. Experimental investigations mainly consist of quenching experiments and a subsequent chemical and/or metallographic analysis, but fail to provide information on the time-dependent evolution of microsegregation during real solidification due to experimental difficulties at elevated temperatures. To remedy this situation, experimental techniques have been developed specifically to study aspects of solidification, which include transmission X-ray observation, the Bridgman furnace and high-temperature laser-scanning confocal microscopy (HTLSCM). Against other *ex-situ* experiments, these techniques provide not only the ability to capture the solidification progress in real time and high resolution but also to observe and measure the morphology and kinetics of phase transformations during solidification. A recently developed experimental setup for HTLSCM [1] has further increased the capabilities of this technique.

The aim of the present work therefore is an attempt to describe the extent of microsegregation during solidification based on the progression of the solidification interface, using HTLSCM. The results of the experimental investigations can be used for a benchmarking against the results of a numerical analysis and various microsegregation models.

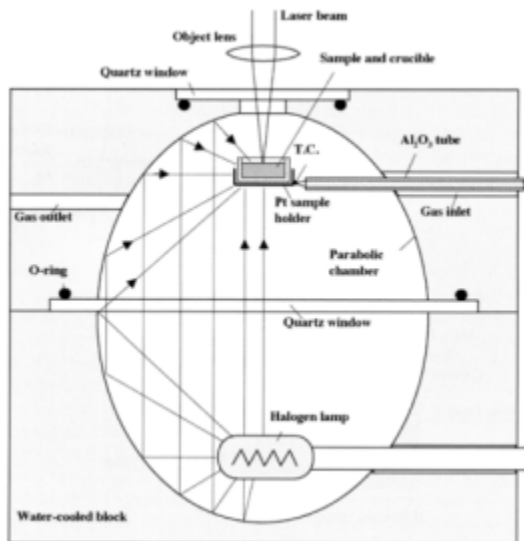
### **1. HTLSCM**

In confocal microscopy, laser light is focused by an objective lens on to the specimen, and the reflected beam is focused onto a photo detector via a beam splitter. In contrast to conventional light microscopy, a confocal microscope uses point-by-point illumination on the specimen and a confocal pinhole in an optically conjugate plane in front of the detector, allowing only light incident from the focal plane to pass through to the photo detector. The out-of-focus signal is blocked by the pinhole and hence, an extremely thin optical section is created, providing a high-resolution image. As only one point of the sample is illuminated at a time, an image is built up by scanning over a regular raster (i.e. a rectangular pattern of parallel scanning lines) of the specimen, which is then stored in an imaging system for subsequent display. Because thermal radiation is also blocked by the confocal pinhole, only the polarized reflection of the high intensity laser beam reaches the imaging sensor and a sharp image is produced. Emi and co-workers [2, 3] were the first to combine confocal microscopy with an

infrared image furnace (IIF) for the *in-situ* study of fine microstructural development at elevated temperatures, which renewed the interest in high temperature microscopy of metals.

In the used system, a He-Ne laser beam with a wavelength of 632.8 nm is scanned two-dimensionally ( $15.7 \text{ kHz} \times 60 \text{ Hz}$ ) and sent through a beam splitter and an objective lens before hitting the surface of the sample. Magnifications up to  $1350\times$  at a resolution of  $0.25 \mu\text{m}$  can be obtained. The sample is placed in a gold plated ellipsoid infrared heating furnace (see Fig. 1 [4]) under an ultra-high purity inert atmosphere,  $>99.9999 \%$  Ar. A 1.5 kW halogen lamp is located at one focal point of the cavity which heats the specimen located at the other focal point. The diameter of the focal point in the centre of the specimen has been experimentally measured to be 2 mm.

Fig. 1 Schematic representation of the infrared furnace used in HTLSCM.

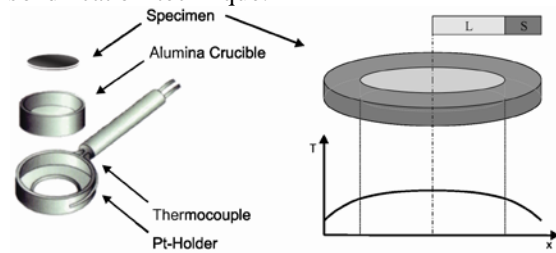


The power input to the halogen lamp is controlled via an OMRON ES100P digital PID controller, which in turn was connected to the thermocouple at the crucible holder for a feedback signal. The temperature as well as the image is simultaneously recorded at a rate of 30 frames per second.

## 1.1 Concentric Solidification

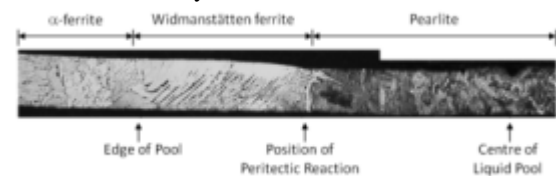
An advanced experimental technique for HTLSCM has been developed by Reid *et al.* [1], which has been utilized for the experiments carried out in this work. It is described as the formation of a centralized pool of liquid metal contained by a rim of solid of the same material under a radial thermal gradient. A specimen of 9.8 mm diameter and about  $250 \mu\text{m}$  thickness is placed in an alumina crucible, which in turn is held in a platinum holder, see Fig. 2. A B-type thermocouple is guided through a 2-bore alumina holding rod and spot-welded on the outer edge of the holder.

Fig. 2 Experimental arrangement for the concentric solidification technique.



The ability to establish a centralized melt pool is dependent upon the existence of a radial thermal gradient across the specimen, whereby the thickness of the sample plays a pivotal role in successfully creating a stable and sustainable liquid pool. It has been established for Fe-C alloys that the maximum sample thickness needs to be  $< 250 \mu\text{m}$  in order to generate a thermal distribution within the specimen beneficial for the formation of a stable liquid pool [1]. A beneficial consequence of using a thin sample is that the through-thickness thermal gradient approaches zero leading to the formation of a vertical solid/liquid interface. This situation can be observed in Fig. 3, where carbon segregation has led to the formation of various microstructural phases along the radial solidification direction in a Fe-0.17 wt.-% C alloy. The significance of this is that observations made of the free surface can be more confidently attributed to events occurring in the bulk as the direction of growth will be primarily in the plane of the specimen. Experimental investigations using cross- as well as planar sectioning of solidified specimen confirm these assumptions. In thick specimens the thermal gradient through the sample thickness is potentially leading to a disturbed liquid–solid interface and uncertainty of the precise direction of growth.

Fig. 3 Cross-section of a concentric solidified Fe-0.17 wt.-% C alloy.



Other benefits of this experimental configuration are the minimization of the meniscus of the melt, resulting in a larger area that is in sharp focus across the solid/liquid interface so that solidification phenomena can be followed over long periods of time without the need for constant refocusing.

Due to the concentric geometry of the phases and the vertical solid/liquid interface an accurate measurement of the fractions of liquid and solid can be carried out for every moment during the experiment. For a known sample radius  $R_S$  and liquid pool radius  $R_P$  the fractions of liquid and solid can be calculated as

$$f_L = (R_p^2 \cdot \pi) / (R_s^2 \cdot \pi) \quad (1)$$

$$f_s = 1 - f_L \quad (2)$$

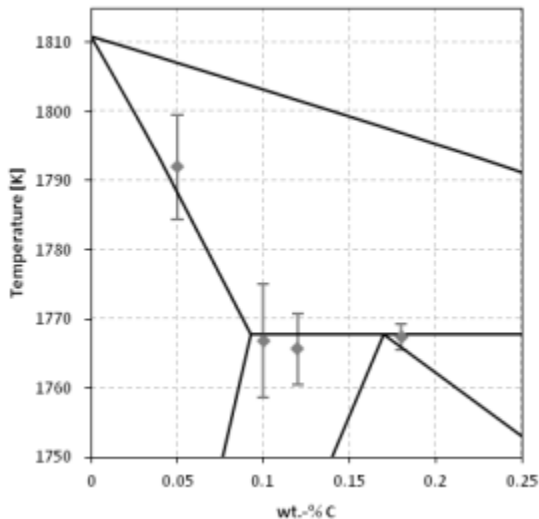
The position of the liquid/solid interface as well as the radius of the liquid melt pool can be automatically determined for every frame by using purposely developed image processing software [5].

## 1.2 Temperature Measurement

In any solidification study it is vitally important to know the exact temperature distribution through the specimen, especially at the advancing solid/liquid interface. Due to the design of the technique, the temperature gradient is a result of the thermal conductivity of the specimen and strongly depending on the fraction of solid. The temperature gradient in the liquid pool is relatively flat due to convection and the high thermal conductivity of the liquid melt, whereas the temperature gradient in the solid is much steeper due to the lower thermal conductivity and heat capacity of the solid.

Experimental experience has revealed a temperature difference of 78.5 °C between the centre of the specimen (i.e. focal point) and the temperature measured at the thermocouple. Fig. 3 shows the experimentally measured melting points for Fe-C alloys with different carbon compositions after a temperature calibration. The measured melting points are in good agreement with the values according to the phase diagram.

Fig. 3 Experimentally measured melting points for different Fe-C alloys after temperature calibration.



In order to assess the temperature at the advancing liquid/solid interface, the phase fractions of solid and liquid can be used to calculate the temperature at the interface by applying the Lever-rule (Fig. 4). It is important to note that this technique is only valid for equilibrium conditions and requires the knowledge of the alloy composition and the correct phase diagram. In the case of the well-known iron-carbon system, which

is in main focus in this work, these assumptions are thought to be valid.

Fig. 4 Schematic illustration of the interface temperature assessment using the phase fractions.

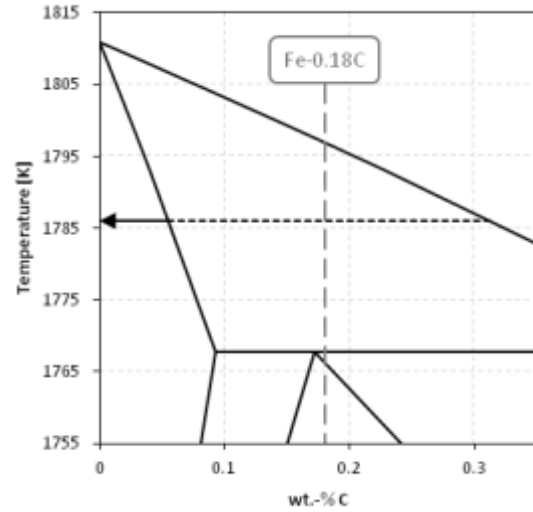
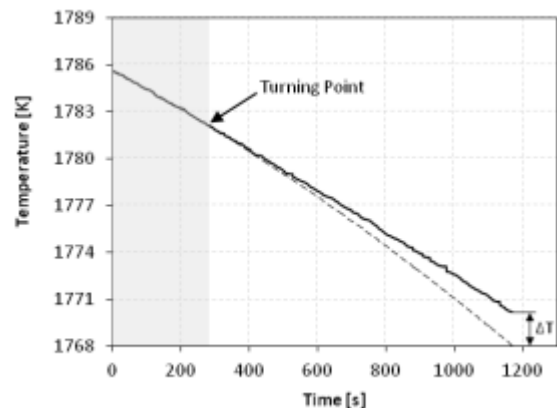


Fig. 5 shows the calculated interface temperature during solidification of a Fe-0.18C alloy with an applied cooling rate of 2 K/min to the peritectic temperature. During initial solidification the interaction between the solute rejection due to partitioning and the solute diffusion in the solid and liquid is such that the conditions are close to equilibrium. The width of the solid rim is small enough to enable sufficient back-diffusion of carbon so that an accurate measurement of the phase fractions can be achieved. The higher the fraction of solid the more time is needed for back-diffusion which leads to the enrichment of solute in the liquid phase and a resulting higher fraction of liquid compared to equilibrium conditions. The application of the Lever-rule to these conditions leads to a higher calculated temperature than the real temperature at the interface (full black line). The transition from close to equilibrium to non-equilibrium conditions can be detected by the localization of the turning point in the temperature versus time plot (Fig. 5).

Fig. 5 Temperature measurement during solidification of a Fe-0.18C alloy.



In order to establish the real interface temperature during the whole experiment, the temperature trend from the initial solidification is extended (dashed line in the temperature-time plot in Fig. 5). The established interface temperature at the moment of the peritectic phase transition is in good agreement with the equilibrium peritectic temperature. Also, the predicted undercooling of 1.3 K below the equilibrium peritectic temperature is in good agreement with the observed kinetics of the peritectic reaction and transformation. The peritectic phase transition turned out to be a good benchmark for the temperature measurement.

## 2. Numerical Analysis

The commercial software package DICTRA [6] has been used to model the concentric solidification experiment. DICTRA is designed to model diffusion controlled transformations in multicomponent alloys by numerically solving the multicomponent diffusion equations:

$$J_k = - \sum_{j=1}^{n-1} \bar{D}_{kj} \frac{\partial c_j}{\partial z} \quad (3)$$

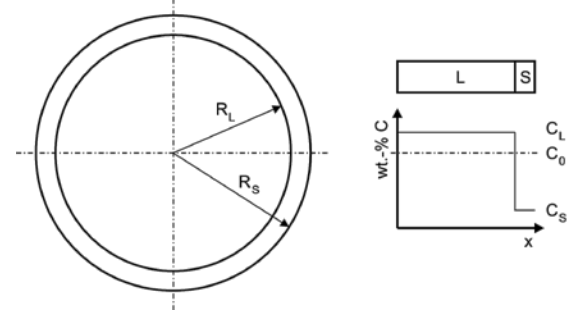
where  $J$  is the resulting solute flux,  $\bar{D}$  the temperature and concentration dependent diffusivity matrix and  $\frac{\partial c}{\partial z}$  the concentration gradient. The moving phase interfaces are calculated by the flux balance under the assumption of local equilibrium at the moving phase interface:

$$\frac{v_m^\alpha}{V_m^\alpha} [x_k^\alpha - x_k^\beta] = J_k^\alpha - J_k^\beta \quad (4)$$

where  $v_m^\alpha$  denotes the interface migration rate,  $V_m^\alpha$  is the molar volume of the  $\alpha$  phase,  $x_k^\alpha$  and  $x_k^\beta$  are the contents of component  $k$  in  $\alpha$  and  $\beta$  close to the phase interface and  $J_k^\alpha$  and  $J_k^\beta$  are the corresponding diffusional fluxes. In DICTRA, diffusion is treated in terms of mobilities and true thermodynamic driving forces, i.e. chemical potential gradients. The thermodynamic functions such as chemical potentials are calculated with Thermo-Calc [7] which runs as a subroutine to DICTRA. The mobility database MOB2 [8] was used covering a large number of elements and phases. The thermodynamic database TCFE6 [9] was used in Thermo-Calc. In order to consider the axisymmetric geometry of the experiment the simulations were carried out using a cylindrical coordinate system. Fig. 6 shows the initial setup for the simulations, similar to the conditions prior to the initiation of solidification in the experiment. The initial liquid pool radius  $R_L$  and the radius of the specimen  $R_S$  were accurately measured in the experiment and adopted to the simulation. Based on the measured phase fractions of solid and liquid, the initial phase concentrations were calculated using the according phase diagram and assigned to the phases in the simulation. The temperature profile was determined

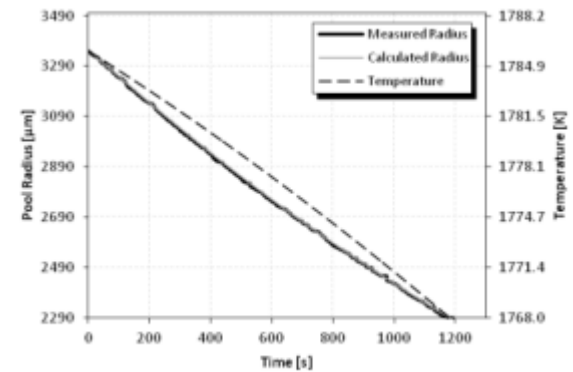
using the aforementioned methodology and applied to the simulation, whereby isothermal conditions have been assumed for the whole domain. The mobility and thermodynamic data necessary for the calculations are stored in databases. The density of the liquid is assumed to be equal to the density of the solid and the thickness of the liquid pool is set equal to the thickness of the solid rim.

Fig. 6 Schematic representation of the initial experimental and simulation setup.



In Fig. 7 a comparison is drawn between the experimentally measured and simulated progression of the liquid/delta-ferrite interface during concentric solidification of a Fe-0.18C alloy. Note that the same temperature profile (dashed line) determined from the experiment (see Fig. 5) has been applied to the simulation.

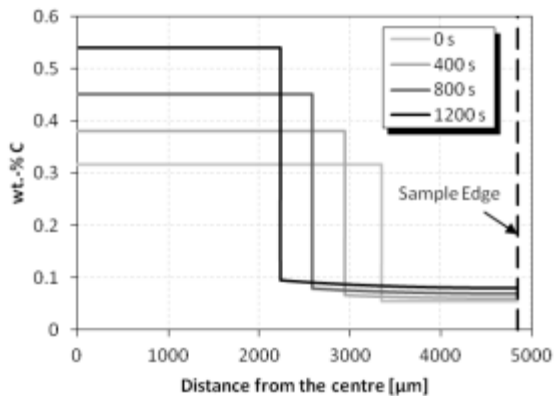
Fig. 7 Measured and simulated liquid/delta-ferrite interface progression for a Fe-0.18C alloy.



The root cause for any interface progression is due to a difference in the chemical potential of the elements across the interface. The chemical potential is strongly depending on the temperature and can simplified be expressed as the concentration of solute elements. The formation of concentration gradients during solidification leads to a flux of the particular element according to Fick's law, causing the progression of the interface. The results of the simulation precisely agree with the experimentally measured values, demonstrating high accuracy of the aforementioned determination of the temperature profile. Additionally, the simulation gives insight in the emerging concentration gradients in the phases during

solidification which cannot be established experimentally, see Fig. 8.

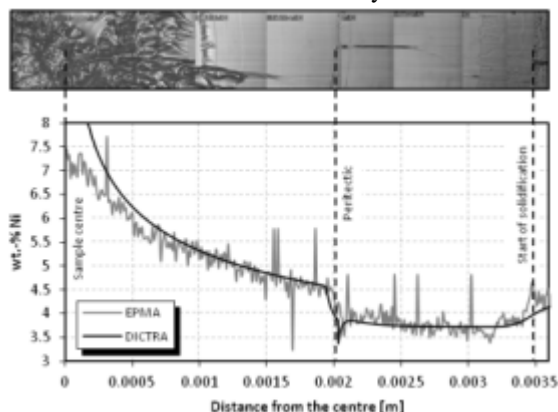
Fig. 8 Simulated concentration profiles during concentric solidification of a Fe-0.18C alloy.



It is important to point out that the simulations have been performed without the presence of any grain boundaries, at which a quantitative difference has to be expected due to the higher diffusivity in these areas.

In order to verify the simulation results, the solute segregation profile of a concentrically solidified Fe-4.2Ni alloy at 5 K/min has been investigated in an earlier work [10] and is presented in Fig. 9. Due to the rapid diffusion of carbon close to the melting point of steel it was not possible to experimentally determine the extent of carbon segregation in samples cooled down to room temperature. Therefore, DICTRA simulations together with concentric solidification experiments of a Fe-4.2Ni alloy were performed in which the solute segregation can be reasonably determined experimentally using EPMA.

Fig. 9 Measured and simulated nickel profile in a concentric solidified Fe-4.2Ni alloy.



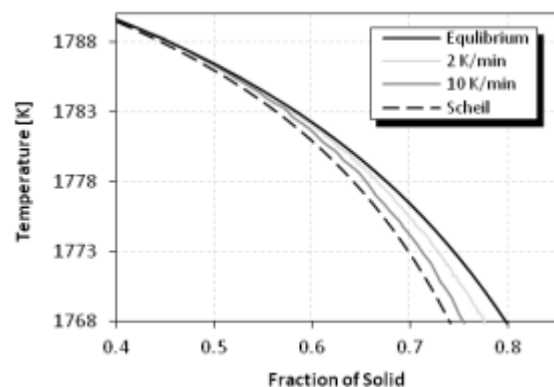
The positions of the solid rim and the peritectic transition are closely matched in the simulation and the actual weight percent of Nickel is well predicted by the simulation.

### 3. Analysis of Microsegregation

The analysis of microsegregation during solidification is based upon the principle of mass conservation in the overall system. By accurately measuring the phase fractions and interface temperature during solidification, a simple mass balance can be used in order to calculate the average compositions in each phase which is then compared to equilibrium conditions and hence, the extent of microsegregation can be quantified.

Fig. 10 shows the interface temperature plotted over the fraction of solid for a concentric solidified Fe-0.18C alloy with a cooling rate of 2 K/min and 10 K/min, respectively. Both of the curves are plotted until the peritectic temperature. The limits for full equilibrium (lever-rule) as well as for conditions where no back-diffusion is allowed (Scheil model) are also plotted for reference. In the case of the lower cooling rate, i.e. 2 K/min, the experimental curve is located close to equilibrium until a fraction of solid of about 0.6. The low cooling rate and the resulting low interface progression rate permits enough time for the partitioned solute elements to diffuse back into the solid rim. The enrichment in the liquid phase is minimal so that the phase fractions remain close to equilibrium conditions. For a fraction of solid higher than 0.6 the experimental curve begins to steadily deviate from the equilibrium boundary. The higher the fraction of solid the more time is needed for back-diffusion and the system becomes metastable.

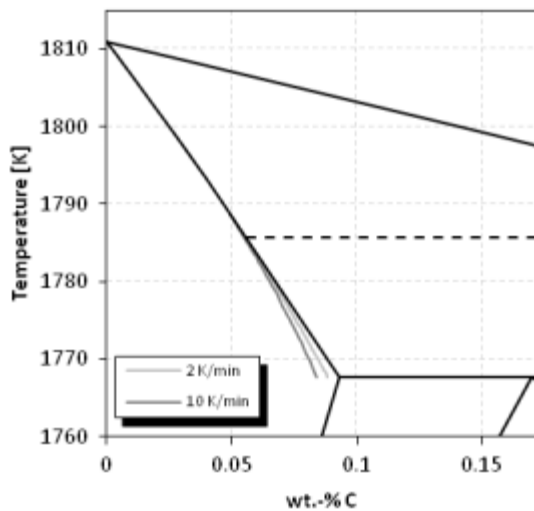
Fig. 10 Microsegregation plot for a Fe-0.18C alloy for different cooling rates.



In the case of the higher cooling rate, i.e. 10 K/min, the experimental curve begins to deviate at a lower fraction of solid compared to the curve representing the lower cooling rate. The propagation of the solidification front occurs at a higher velocity reducing the time for sufficient back-diffusion, resulting in an enrichment of the liquid phase and a decreasing fraction of solid for a given temperature compared to equilibrium conditions.

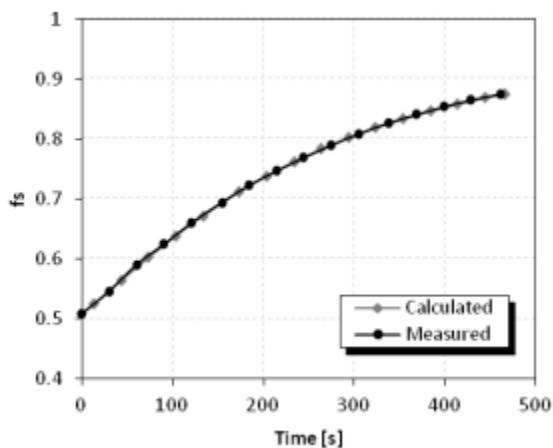
The average phase concentrations can be calculated by comparing the measured phase fractions to the phase fraction under equilibrium conditions (Lever rule), as it is shown in Fig. 11 for both cooling rates.

Fig. 11 Average solid compositions during concentric solidification of a Fe-0.18C alloy.



For the analysis of microsegregation in ternary systems, the distribution of the solute elements can be calculated by coupling DICTRA with the experimentally measured parameters in HTLSCM (e.g. temperature profile). Fig. 12 shows the increase of solid fraction over time during solidification of a Fe-0.13C-0.5Si alloy with 10 K/min as well as the result of the DICTRA simulation. Because the interface progression can precisely be modelled in DICTRA, and its strong dependency on the concentration and temperature profiles, the concentration profiles resulting from the DICTRA simulations can be taken for a further analysis.

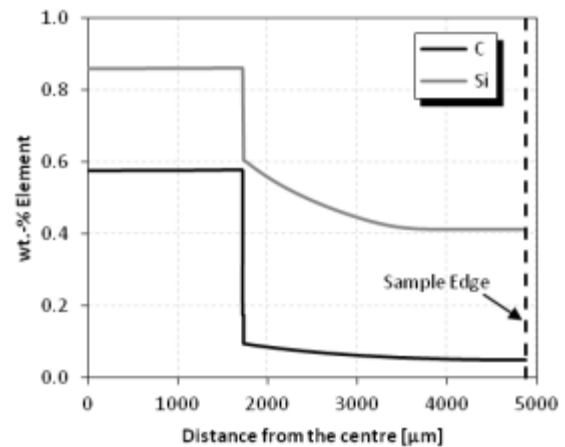
Fig. 12 Interface progression over time for a Fe-0.13C-0.5Si alloy solidified with 10 K/min.



In Fig. 13 the concentration profiles are shown for silicon and carbon at the peritectic temperature for a

Fe-0.13C-0.5Si alloy concentrically solidified with a cooling rate of 10 K/min.

Fig. 13 Concentration profiles at the peritectic temperature in a Fe-0.13C-0.5Si alloy.



As expected, the silicon profile shows a much steeper gradient compared to the carbon profile due to the different diffusivities of the elements.

## Conclusions

We present a method for the *in-situ* quantification of microsegregation that occurs during the solidification of steel. A recently developed sample geometry for HTLSCM has been utilized to perform solidification experiments under controlled conditions. The concentric geometry of the specimen allows a very accurate measurement of the phase fractions during solidification, which were automatically measured using purposely developed image processing software. The temperature at the liquid/solid interface was determined by a temperature calibration, which enabled the calculation of the effective cooling rate at this interface. By comparing the measured phase fractions to the equilibrium phase fractions at a given temperature, the average composition of the phases was calculated and the extent of microsegregation quantified.

The results of a numerical analysis of the interface progression during solidification using DICTRA were in very good agreement with the experimental measurements, allowing a detailed analysis on the emerging concentration gradients during solidification. However, even though a first validation was shown to be successful (see Ref. [10]), a further experimental validation of the element distribution needs to be done for systems with a higher number of alloying elements for a final validation of the technique.

## Acknowledgement

Financial support by the Austrian Federal Government (in particular from the Bundesministerium für Verkehr, Innovation und Technologie and the Bundesministerium für

Wirtschaft und Arbeit) and the Styrian Provincial Government, represented by Österreichische Forschungsförderungsgesellschaft mbH and by Steirische Wirtschaftsförderungsgesellschaft mbH, within the research activities of the K2 Competence Centre on “Integrated Research in Materials, Processing and Product Engineering”, operated by the Materials Center Leoben Forschung GmbH in the framework of the Austrian COMET Competence Centre Programme, is gratefully acknowledged by one of the authors (SG).

## References

1. Reid M.; Phelan D.; Dippenaar R.J.: ISIJ International, 2004, 44(3), pp 565–572.
2. Chikama H.; Shibata H.; Emi T.; Suzuki M.: Mater. T. JIM, 1996, 37(4), pp 620–626.
3. Yin H.; Emi T.; Shibata H.: ISIJ Int., 1998, 38(8), pp 794–801.
4. Cantor B.; O’Reilly K.: Solidification and Casting, IOP Publishing Ltd, London, 2003.
5. Griesser S.; Pierer R.; Reid M.; Dippenaar R.: Journal of Microscopy, in review.
6. Andersson J.-O., Höglund L., Jönsson B., Ågren J.: Fundamentals and Applications of Ternary Diffusion, Ed. By G. R. Purdy, Pergamon Press, New York, 1990, pp 153-163.
7. Sundman B., Jansson B., Andersson J.-O.: CALPHAD, 1985, 9, pp. 153–90.
8. MOB2, Mobility Databases, Thermo-Calc Software AB, Stockholm.
9. TCFE6, Steels/Fe-alloys databases, Thermo-Calc Software AB, Stockholm.
10. Aminorroaya S., Reid M., Dippenaar R.: Modelling Simul. Mater. Sci. Eng., 2011, 19, 025003 (16pp).